

Formation and evolution of the transverse anisotropy with nanocrystallization in amorphous $\text{Fe}_{73.5}\text{CuNb}_3\text{Si}_{13.5}\text{B}_9$ ribbons

H. Q. Guo,^{1,2} H. Kronmüller,² T. Dragon,² Z. H. Cheng,^{1,2} and B. G. Shen¹

¹State Key Laboratory of Magnetism, Institute of Physics & Centre of Condensed Matter Physics, Chinese Academy of Sciences, Beijing 100080, People's Republic of China

²MPI für Metallforschung, D-70506 Stuttgart, Germany

(Received 27 January 2000)

The evolution of the magnetic domain patterns has been studied in amorphous $\text{Fe}_{73.5}\text{CuNb}_3\text{Si}_{13.5}\text{B}_9$ ribbons by suitable "long duration" thermal treatments. It is shown that by annealing at 550 °C for annealing time t_a from 1 to 150 h, very fine nanocrystalline bcc-FeSi grains are homogeneously formed in the amorphous matrix. Although with increasing t_a the grain size remains very fine (≤ 11 nm), the coercivity H_c increases rapidly from 0.14 A/m for $t_a = 3$ h to 133 A/m for $t_a = 150$ h. For the nanocrystalline ribbons with $t_a = 3$ h, the domain structure is characterized by a few broad longitudinal together with some broad transverse domain patterns, connected to the minimum coercive field. With increasing annealing time $t_a \geq 10$ h, only transverse domain patterns are observed and the transverse domain width gradually becomes narrow. By applying an external magnetic field, the magnetization processes indicate that the easy magnetization may lie between the longitudinal and transverse directions for the samples annealed for $t_a = 1, 3,$ and 10 h, while in the sample of $t_a = 30$ h, the easy magnetization in domains is transverse to the ribbon direction. The induced transverse anisotropy of 380 J/m³ in the sample of $t_a = 30$ h is determined from the domain width. The estimated H_c for the coherent rotation process in the sample of $t_a = 30$ h is compatible with the experimentally observed value.

In 1988 Yoshizawa, Oguma, and Yamauchi¹ reported a new class of iron-based alloys with excellent soft magnetic properties, which is formed after devitrification when annealed at the optimum temperature. This kind of soft material consists of nanocrystallites randomly nucleated in a soft amorphous matrix. The alloy composition originally proposed and subsequently not much changed is $\text{Fe}_{73.5}\text{CuNb}_3\text{Si}_{13.5}\text{B}_9$ at. %. Based on the random anisotropy model,² Herzer³ has shown that the magnetic softness is related to the ratio of the exchange correlation length L (or domain wall thickness) to the average crystallite size δ . For $L \gg \delta$ the magnetocrystalline anisotropy is averaged out and the domain wall can move without hindrances. In addition, the resulting magnetoelastic anisotropy is very small, since for a critical crystallized volume fraction x , the average magnetostriction vanishes.

The investigation of the domain structure and magnetization processes is particularly important for the further improvement of the soft magnetic properties of these materials. Previous observations⁴⁻⁶ have shown that the domain structures of these materials with very high permeability are characterized by large domains divided by 180° walls, the outstanding soft magnetic properties seem to be connected to the extremely high mobility of the few domain walls present. On annealing beyond the optimum temperature the magnetic softness deteriorates which manifests itself with irregular domain appearance. In the present work we have investigated the evolution of domain patterns and the corresponding magnetization processes upon long duration treatment at 550 °C in the $\text{Fe}_{73.5}\text{CuNb}_3\text{Si}_{13.5}\text{B}_9$ alloy. With increasing annealing time t_a a gradually change of transverse domain width and transition of magnetization processes are observed in this nanocrystalline alloy. The observed degradation of soft prop-

erties before the influence of the increased grain size is attributed to the increase of the transverse anisotropy, which is supposed to be originated from the new stresses developed during nanocrystals formation.

The amorphous $\text{Fe}_{73.5}\text{CuNb}_3\text{Si}_{13.5}\text{B}_9$ ribbons, 30 μm thick and 10 mm wide, were produced by single-roller rapid quenching in the Institute of Physics of the Slovak Academy of Sciences at Bratislava. The ribbons were cut in strips, 1.5 mm wide and 50 mm long. For annealing procedure, we put a quasiboat with one strip sample in a quasitube, and then vacuumize the quasitube up to 10^{-6} Torr. After the temperature in a furnace reaches 550 °C, the quasitube was moved into the furnace and kept in it without magnetic field for some time, for instance, for 1 or 3 h and up to 150 h. And then the quasitube was taken out from the furnace and cooled in the air. The coercivity H_c of the annealed samples were first measured in an earth-field-compensated solenoid using a Förster coercimeter. The domain pattern observations on the same samples were made by magneto-optical Kerr effect microscopy. At last, the microstructure was determined by transmission electron microscopy (TEM) and x-ray diffraction with rotating anode (Rigaku D/max2400). Figure 1 gives TEM micrographs and the corresponding electron diffraction patterns for the sample annealed at 550 °C for 1 and 150 h, respectively. As demonstrated in Fig. 1, very fine nanocrystalline grains are homogeneously embedded into an amorphous matrix. Upon annealing time t_a from 1 to 150 h, the grain size changes very little, varying from about 9 to 11 nm. From temperature dependence of the specific magnetization σ_s , the weight percent W_α of bcc-FeSi phase is determined by the $\sigma^{1/\beta} - T$ plot method.³ For the sample annealed for 1 h, the weight percent W_α of the bcc-FeSi phase is about 75%. With increasing annealing time t_a , the Curie

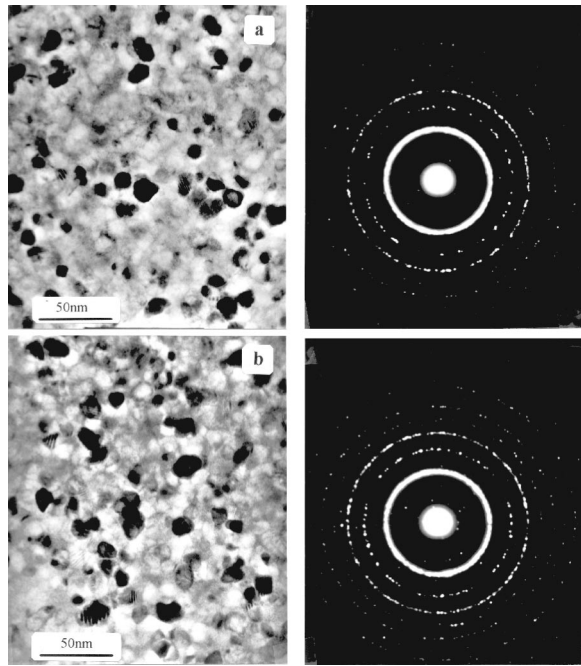


FIG. 1. TEM micrograph and electron diffraction patterns of nanocrystalline $\text{Fe}_{73.5}\text{CuNb}_3\text{Si}_{13.5}\text{B}_9$ ribbons: (a) annealed at 550°C for 1 h, (b) for 150 h.

temperature of the bcc-FeSi phase keeps nearly the same, about 600°C , but the irregular bend observed in the $\sigma_s(T)$ curves is less noticeable due to increasing crystallized fraction and disappears for the sample annealed for 30 h, corresponding to the end of the first crystallization stage. The samples in strip form were step scanned with Cu radiation at Bragg angle 2θ ranging from 40° to 125° (with step of 0.02° , 1 s). The step-scanned x-ray spectra after elimination of $K_{\alpha 2}$ as shown in Fig. 2, indicates noncrystalline texture of the α -FeSi grains in the annealed samples. With increasing t_a the

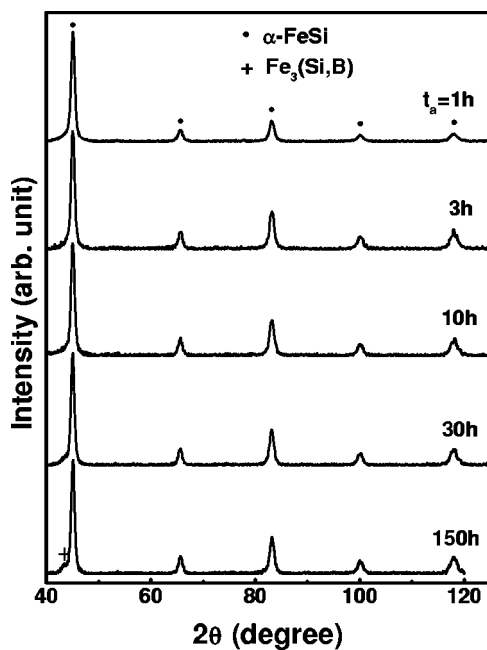


FIG. 2. Step-scanned x-ray spectra of $\text{Fe}_{73.5}\text{CuNb}_3\text{Si}_{13.5}\text{B}_9$ ribbons annealed at 550°C for $t_a = 1$ to 150 h.

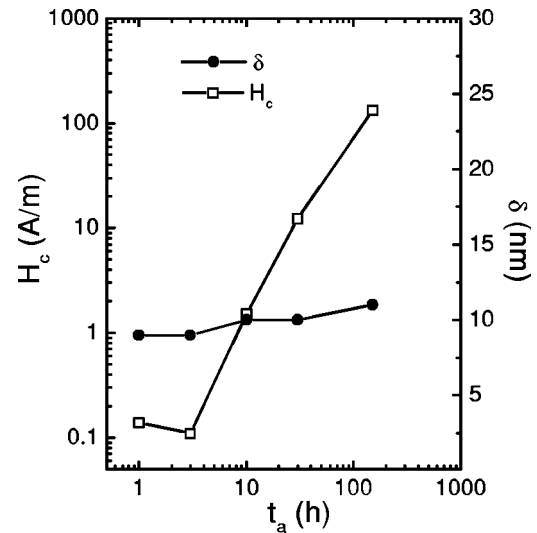


FIG. 3. The annealing time dependence of H_c and grain size with t_a for the $\text{Fe}_{73.5}\text{CuNb}_3\text{Si}_{13.5}\text{B}_9$ ribbons.

lattice parameter, obtained from x-ray diffraction spectra, changes slightly from 0.2841 nm for 1 h to 0.2843 nm for 150 h, which is compatible with the value obtained by Yoshizawa.¹ For the sample annealed for $t_a = 150\text{ h}$, the x-ray diffraction spectrum shows a small additional line with interplanar spacing of 0.2081 nm , which corresponds to the diffraction pattern (220) of the orthorhombic $\text{Fe}_3(\text{Si},\text{B})$ phase. Figure 3 shows the dependence of coercivity H_c and grain size on the annealing time t_a . It is shown that for $t_a > 3\text{ h}$, H_c changes its values rapidly with t_a by several orders of magnitude, even though the grain size δ , is still much smaller than the exchange correlation length L (35 nm).⁷ The deterioration of the magnetic softness before growth of the FeSi grains was also observed^{5,8} previously in this materials, which leads to invalidity of the δ^6 dependence of H_c deduced from the simplified model made by Herzer.³

Figure 4 presents the evolution of domain patterns of amorphous and nanocrystalline FeCuNbSiB ribbons in the demagnetized state. For the amorphous sample, it is well known that the wide and wavy laminae patterns as well as the narrow laminar patterns in Fig. 4(a), as observed also in other amorphous alloys,⁹ are generated by tensile and compressive stresses, respectively, produced by the rapid quenching process. For the nanocrystalline ribbons with shorter annealing $t_a = 1, 3,$ and 10 h broad transverse domain patterns are dominant as observed in Figs. 4(b)–4(d). For $t_a > 10\text{ h}$ the transverse domain width D_0 gradually becomes narrow with increasing annealing time. Under an applied magnetic field H_{ext} parallel or transverse to the ribbon direction the magnetization processes for the samples with various t_a are distinguishable. For instance, in samples with $t_a = 1, 3,$ and 10 h , applying a small external magnetic field in the direction parallel to the ribbon direction results in a domain wall displacement of the transverse domains (Fig. 5), which is the dominant contribution to the change of magnetization in the initial magnetization processes. And even if the magnetic field is applied transverse to the ribbon axis, domain wall movements are still observed, as shown in Fig. 5. This implies that the easy magnetization in transverse domain may lie between the longitudinal and transverse direc-

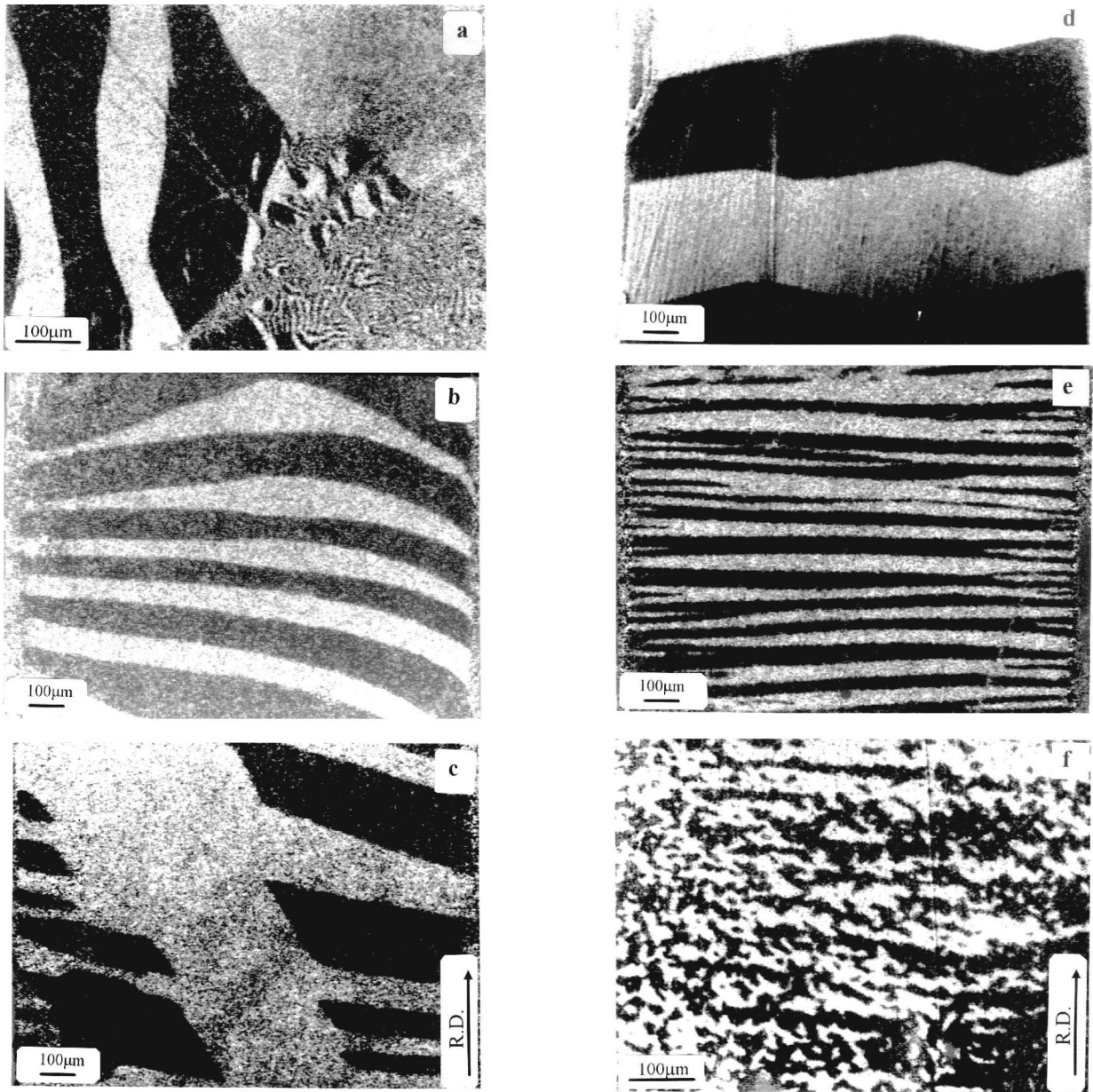


FIG. 4. Domain patterns of $\text{Fe}_{73.5}\text{CuNb}_3\text{Si}_{13.5}\text{B}_9$ ribbons in the demagnetised state: (a) asquenched, (b) annealed at 550°C for $t_a = 1$ h, (c) $t_a = 3$ h, (d) $t_a = 10$ h, (e) $t_a = 30$ h, (f) $t_a = 150$ h.

tions for these samples. Figure 6 shows narrow and regular transverse domain patterns of the sample with $t_a = 30$ h. After applying a longitudinal magnetic field the contrast between the domains keeps decreasing until the domain patterns vanish, which results from a homogeneous rotation of the magnetization within the domains, while under a transverse magnetic field only domain wall movement occurs. This indicates that the easy magnetization directions is transverse to the ribbon direction. For the sample with $t_a = 150$ h only changes of the contrast between the very fine and discontinuous transverse domains are observed in both longitudinal and transverse applied fields due to rotation process of magnetization in domains.

Recently, based on the random anisotropy approximation, Hernando *et al.*¹⁰ have established a simple phenomenological theory, which takes into account the two-phase character of nanocrystalline materials. According to this theory, the

total anisotropy, provided $\delta < \delta^*$ holds, is given by

$$K_t = xK_0 / \gamma^3 + 3\lambda_{\text{ef}} \langle \sigma \rangle / 2, \quad (1)$$

where the first term is a structural anisotropy K_s in the crystallized volume fraction x , a parameter γ varying between 0 and 1, the macroscopic anisotropy of single phase, $K_0 = (3/4)^3 \delta^6 k^4 / A^3$ with the average crystallite size δ , uniaxial anisotropy constant k of the nanocrystals and the strength A of the exchange interactions between any pair of adjacent nanocrystals and the maximum size of crystallites $\delta^* = (A/k)^{0.5} \gamma / x^{2/3}$; the second one is the magnetoelastic anisotropy with effective magnetostriction constant $\lambda_{\text{ef}} = \lambda_c x + \lambda_{\text{am}}(1-x)$, where λ_c is magnetostriction for nanocrystals and λ_{am} for amorphous matrix, and the average absolute value of stresses $\langle \sigma \rangle$, which is expected to change with the thermal treatments through either stress relaxation of the

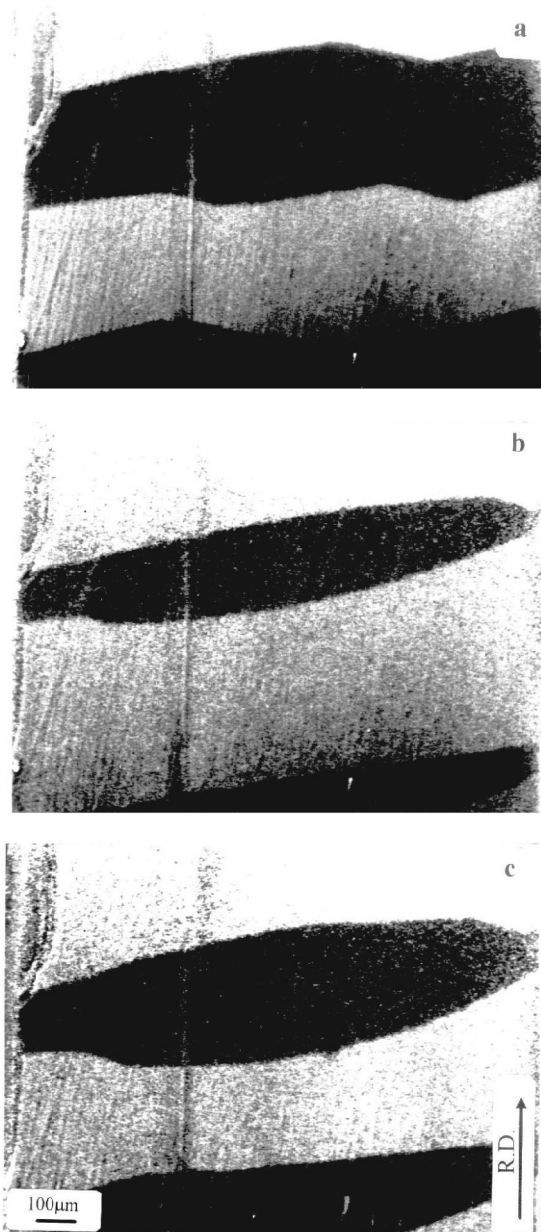


FIG. 5. Domain patterns of a nanocrystalline ribbon (annealed at 550 °C for 10 h): (a) in the demagnetized state (b) in the applied longitudinal magnetic field of $H_{\text{ext}}=0.42$ Oe, (c) in the applied transverse magnetic field of $H_{\text{ext}}=48.8$ Oe.

amorphous structure for annealing temperatures below the onset of crystallization, or by the stress developed during nanocrystals formation within the amorphous matrix. For the samples with $t_a=1-30$ h, the grain size δ is much smaller than the exchange correlation length, e.g., $\delta \ll L$ (35 nm),⁷ the macroscopic structural anisotropy K_s averages out to be about 14 J/m³ (Ref. 8), and the slight change in grain size and the crystalline fraction with t_a should not have a substantial influence on the macroscopic structural anisotropy. So the K_s losses the importance in the K_t and the change of the total anisotropy K_t with t_a is mainly attributed to that of the magnetoelastic anisotropy K_e , which has two contributions of opposite sign, coming from crystalline and from the residual amorphous matrix. For the sample annealed for $t_a=1$ h, the transverse domain patterns is similar to that ob-

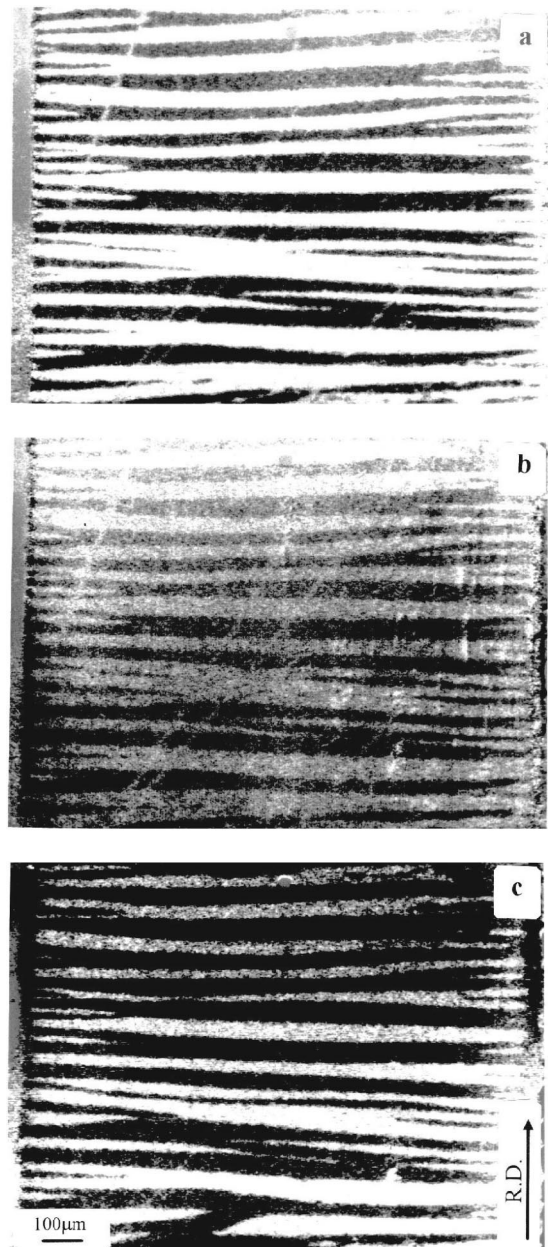


FIG. 6. Domain patterns of a nanocrystalline ribbon (annealed at 550 °C for 30 h): (a) in the demagnetized state, (b) in the external longitudinal magnetic field of $H_{\text{ext}}=6.2$ Oe, (c) in the external transverse magnetic field of $H_{\text{ext}}=87.8$ Oe.

served in Fe-based annealed amorphous ribbons.⁹ It is likely that the magnetoelastic anisotropy in this sample is not completely compensated when nanocrystallization takes place. As Franco *et al.* claimed,¹¹ in addition to the residual internal stresses, new stresses developed by nanocrystals formation is also the origin of the magnetoelastic anisotropy. But for the sample annealed for $t_a=3$ h, a few wide longitudinal domains appear together with wide transverse domains. As observed by Hofmann,⁸ This domain structure takes place in the case of optimal annealing condition, under which the two opposite contributions to the magnetoelastic anisotropy are the best compensated, leading to minimum H_c and K_t . With further increasing t_a , a transverse anisotropy is developed in the sample of $t_a=10$ h. Especially, for $t_a \geq 10$ h the K_u increases evidently with t_a according to the domain width D_0

$\sim K_u^{-1/4}$.⁹ For the sample annealed for $t_a=30$ h, which possesses typical transverse domain patterns with magnetization in the transverse direction to the ribbon axis, the anisotropy K_u of about 380 J/m^3 is determined from the relation of $K_u = 64AT_o^2/D_o^4$,⁹ with the exchange constant $A=10^{-11} \text{ J/m}$,⁷ the ribbon width $T_o=1.5 \text{ mm}$ and the domain width $D_o=44 \mu\text{m}$. Using the results for coherent spin rotation,¹² the H_c of 35 A/m is estimated from $H_c=p_c K_u/J_s$ where $p_c=0.13$,⁷ $J_s=1.25 \text{ T}$,³ which is close to the experimentally observed value. With regard to the origin of the degradation of good magnetic properties, or the induced transverse anisotropy in the samples of $t_a=10$ and 30 h there are several possible causes for analysis. (1) Changes of the silicon content in $\alpha\text{-FeSi}$ phase can strongly influence magnetic properties owing to changes in magnetocrystalline anisotropy and magnetostriction, as observed by Duhaj *et al.*¹³ A very small change of about 2 at. % in the silicon content in $\alpha\text{-FeSi}$ phase, deduced from the small change of the lattice parameters for the samples from $t_a=1$ to 150 h, cannot cause so

large changes of H_c or anisotropy, (2) It is well known that the precipitation of boride-type phases with high anisotropy degrades the soft properties. But borides precipitation has not been detected in the samples annealed for $t_a=10$ and 30 h, (3) Consequently, it is plausible to presume that the new stresses developed during nanocrystals formation are dominant contributions to the magnetoelastic anisotropy. The formation mechanism of the induced anisotropy still needs to be studied further. The domain patterns of the sample with $t_a=150$ h is similar to that observed in the sample annealed at 620°C .⁸ In this sample precipitation of the new $\text{Fe}_3(\text{Si},\text{B})$ phase with high anisotropy, as a strong pinning of domain walls prevents a magnetization by domain displacements.

The authors thank B. Ludescher, A. Neuweiler, and W. Maisch for their assistance in the experiments and M. Kelsch for the TEM micrograph. This work was supported by the State Key Project of Fundamental Research and the National Science Foundation of China.

¹Y. Yoshizawa, S. Oguma, and K. Yamauchi, *J. Appl. Phys.* **64**, 6044 (1988); **64**, 6047 (1988).

²R. Alben, J. J. Becker, and M. C. Chi, *J. Appl. Phys.* **49**, 1653 (1978).

³G. Herzer, *IEEE Trans. Magn.* **25**, 3327 (1989); *Mater. Sci. Eng., A* **133**, 1 (1991); *Phys. Scr.* **T39**, 307 (1993).

⁴R. Schafer, A. Hubert, and G. Herzer, *J. Appl. Phys.* **69**, 5325 (1991).

⁵T. Reininger, B. Hofmann, and H. Kronmüller, *J. Magn. Magn. Mater.* **111**, L220 (1992).

⁶K. Zaveta and Z. Kalva, in *Nanomagnetism*, Vol. 247 of *NATO Advanced Studies Institute, Series E: Applied Sciences* (Plenum, New York, 1993), p. 247.

⁷G. Herzer, *IEEE Trans. Magn.* **26**, 1397 (1990).

⁸B. Hofmann, T. Reininger, and H. Kronmüller, *Phys. Status Solidi A* **134**, 247 (1992).

⁹H. Kronmüller, M. Fähnle, M. Domann, H. Grimm, R. Grimm, and B. Groger, *J. Magn. Magn. Mater.* **13**, 53 (1979).

¹⁰A. Hernando, M. Vazquez, T. Kulik, and C. Prados, *Phys. Rev. B* **51**, 3581 (1995).

¹¹V. Franco, C. F. Conde, and A. Conde, *J. Magn. Magn. Mater.* **185**, 353 (1998).

¹²R. M. Bozorth, *Ferromagnetism* (Van Nostrand, Princeton, 1951), Chap. 18, pp. 811–837.

¹³P. Duhaj, P. Švec, D. Janičkovič, I. Matko, and M. Hlášnik, *Mater. Sci. Eng., B* **14**, 357 (1992).